Biochemical and Biophysical Research Communications 430 (2013) 769–773

Contents lists available at SciVerse ScienceDirect

Biochemical and Biophysical Research Communications

journal homepage: www.elsevier.com/locate/ybbrc

Zinc ion coordination as a modulating factor of the ZnuA histidine-rich loop flexibility: A molecular modeling and fluorescence spectroscopy study

Silvia Castelli [a], Lorenzo Stella [b,c], Patrizia Petrarca [a], Andrea Battistoni [a,e], Alessandro Desideri [d,e], Mattia Falconi [d,e,*]

[a] Department of Biology, University of Rome Tor Vergata, Via della Ricerca Scientifica, 00133 Rome, Italy
[b] Department of Chemical Sciences and Technologies, University of Roma Tor Vergata, Via della Ricerca Scientifica, 00133 Rome, Italy
[c] Neuromed, IRCCS, Pozzilli (IS) 86077, Italy
[d] Department of Biology, University of Rome Tor Vergata and CIBB, Center of Biostatistics and Bioinformatics, Via della Ricerca Scientifica, 00133 Rome, Italy
[e] Interuniversity Consortium, National Institute Biostructure and Biosystem (INBB), Viale delle Medaglie D'Oro 305, 00136 Rome, Italy

ARTICLE INFO

Article history:
Received 7 November 2012
Available online 1 December 2012

Keywords:
Fluorescence spectroscopy
Protein labeling
Molecular modeling
Zinc transport
ABC transporter

ABSTRACT

ZnuA is the soluble component of the high-affinity ZnuABC zinc transporter belonging to the ATP-binding cassette-type periplasmic Zn-binding proteins. The zinc transporter ZnuABC is composed by three proteins: ZnuB, the membrane permease, ZnuC, the ATPase component and ZnuA, the soluble periplasmic metal-binding protein which captures Zn and delivers it to ZnuB.

The ZnuA protein contains a charged flexible loop, rich in histidines and acidic residues, showing significant species-specific differences. Various studies have established that this loop contributes to the formation of a secondary zinc binding site, which has been proposed to be important in the acquisition of periplasmic Zn for its delivery to ZnuB or for regulation of zinc uptake. Due to its high mobility the structure of the histidine-rich loop has never been solved by X-ray diffraction studies. In this paper, through a combined use of molecular modeling, mutagenesis and fluorescence spectroscopy, we confirm the presence of two zinc binding sites characterized by different affinities for the metal ion and show that the flexibility of the loop is modulated by the binding of the zinc ions to the protein. The data obtained by fluorescence spectroscopy have then be used to validate a 3D model including the unsolved histidine-rich loop.

1. Introduction

Transition metals play key roles in all organisms mainly because they serve as essential cofactors in a large number of proteins. Among such metals zinc is likely the most abundantly used in enzymes and bioinformatics analyses have suggested that it is contained in at least 5% of bacterial and about 9% of eukaryotic proteins [1,2].

Recent studies have begun to elucidate the mechanisms by which bacteria control the amount of intracellular zinc [3]. In particular, it has been established that several bacteria respond to zinc deficiency by expressing the ZnuABC high affinity zinc uptake system, a transporter of the ABC family whose expression is repressed by the metallated form of the regulatory protein Zur [4]. This transporter includes three proteins: the soluble periplasmic protein ZnuA, the ZnuB membrane channel and the ATPase component ZnuC.

In addition, in some bacteria the activity of ZnuABC is supported by another zinc-binding protein, ZinT, which collaborates with ZnuA in the recruitment of zinc in the periplasmic space [5]. Deletion of the genes encoding for ZnuABC not only decreases the ability of different bacteria to grow in media poor of zinc, but has a dramatic effect on the ability of pathogens to colonize the host and cause disease [6]. For example, studies carried out with *Salmonella enterica* have established that ZnuABC is highly expressed in intracellular environments [6] and that this zinc transporter favors *Salmonella* proliferation in the inflamed gut, as it overcomes calprotectin-mediated zinc-sequestration, thus allowing *Salmonella* growth over the intestinal microbiota [7]. Interestingly, the absence of ZnuA is sufficient to completely inhibit zinc import through ZnuB [5], thus suggesting that strategies aimed at blocking this transporter may be useful to control pathogens proliferation.

ZnuA belongs to the cluster 9 of bacterial periplasmic binding proteins, which includes proteins able to specifically bind zinc or manganese [8]. The crystal structures of ZnuA from *Synechocystis* sp. 6803 [9], *Escherichia coli* [10] and *S. enterica* [11], show a well conserved structure characterized by two (α/β)4 domains connected by a long and flexible α-helix. A primary high-affinity metal

* Corresponding author at: Department of Chemical Sciences and Technologies, University of Roma Tor Vergata, via della Ricerca Scientifica, 00133 Rome, Italy. Fax: +39 06 2022798.
E-mail address: falconi@uniroma2.it (M. Falconi).

0006-291X/$ - see front matter © 2012 Elsevier Inc. All rights reserved.
http://dx.doi.org/10.1016/j.bbrc.2012.11.073

binding site is located in the cleft between the two domains. Moreover, these proteins are characterized by a long and mobile histidine-rich loop (His-loop), whose structure has never been fully characterized through crystallographic studies, which protrudes from the protein structure and localizes close to the primary metal binding site. This protein region may bind zinc with significant lower affinity with respect to the primary site [10,12,13]. Structural–dynamical investigations have confirmed that this loop is highly mobile and have suggested that its fluctuations may be influenced by zinc binding either in the primary site or in the His-loop itself [14].

Different roles have been proposed for this His-rich region, including that of facilitating zinc binding in a competitive environment [15] or to regulate zinc import by sensing high periplasmic levels of zinc [12]. In vivo studies on mutant ZnuA lacking the His-rich region have shown that ZnuA may transport zinc also in the absence of this metal-binding domain, but that it helps in recruiting zinc under conditions of severe zinc depletion in the absence of ZinT, thus supporting the hypothesis that it has a role in favoring zinc uptake [5].

In most of the ZnuA structures resolved so far zinc is coordinated in the primary site by three conserved histidine residues and a water molecule or a glutamic acid as a fourth ligand. Whereas the same coordination may be likely assumed also by *S. enterica* ZnuA [14], the crystal structure of this protein has revealed a distinct metal coordination involving a His residue from the mobile His-loop and it has been suggested that this peculiar metal coordination may be favored by low metal occupancy [11]. These findings suggest that the two metal binding regions may be correlated and that the His-loop may have a direct role in zinc transport, either by facilitating zinc transfer from the His-loop to the primary metal binding site or from ZnuA to ZnuB.

In order to deepen the knowledge on the relationships between the two zinc metal binding sites of ZnuA and on the effects of the metal on the structure of the His-loop, molecular modeling and fluorescence spectroscopy studies have been carried out on wild-type ZnuA and on a mutant bearing a fluorophore attached to a central residue of the His-loop. In this research we confirm, using a different approach, that zinc binds with low affinity to the His/acid loop [12] and, investigating the structural/functional consequences of zinc binding on the protein structure and the relationships between the two binding sites, we propose a novel functional role for the ZnuA His-loop.

2. Materials and methods

2.1. ZnuA modeling

One of the two ZnuA models, modeled as previously described with a loaded secondary zinc site located in the His-loop [14], has been used to plan the fluorescence spectroscopy experiments and to explain their results. We have chosen to use a model of the *S. enterica* ZnuA, rather than its available X-ray structure [11], because in that structure, due to its high mobility, the His-loop is absent with the exception of a short segment containing an histidine coordinating the metal. This particular ligand arrangement [11] may correspond to a ZnuA transient intermediate in which the zinc is transferred from the His-loop to the primary metal binding site, but it is not suitable to explain the results of our fluorescence experiments. The model used to elucidate the spectroscopic results contains two metal ions in two different zinc sites: the zinc ion in the primary site maintains the ligands Glu59, His60, His147 and His211, already described in the *E. coli* X-ray diffraction [10], while the secondary zinc ion, easily modeled thanks to the plasticity of the histidine-rich loop, was arbitrarily bound to residues Glu132, Asp136, His141 and His228 [14], this latter conserved as a zinc ligand based on the Yatsunyk and coworkers experimental evidence [10].

2.2. Protein mutation and purification

In order to selectively attach a fluorescent label, *Salmonella typhimurium* ZnuA (StZnuA) has been mutated at the residue Ala130 in cysteine (StZnuA Ala130Cys) (Fig. 1A). This residue has been chosen for its favorable position, located in the middle of the His-loop, and for its particularly low average fluctuation (Root Mean Square Fluctuations, RMSF) detected by molecular dynamics simulation in the models, containing two coordinated zinc ions [14]. In fact, for any possible zinc coordination within the His-loop, a fluorophore bound to residue 130 should be able to sense the association process.

Single-site mutation Ala130Cys was generated by oligonucleotide-directed mutagenesis (QuikChange site-directed mutagenesis kit Stratagene Cloning Systems) of the p18PznuA expression

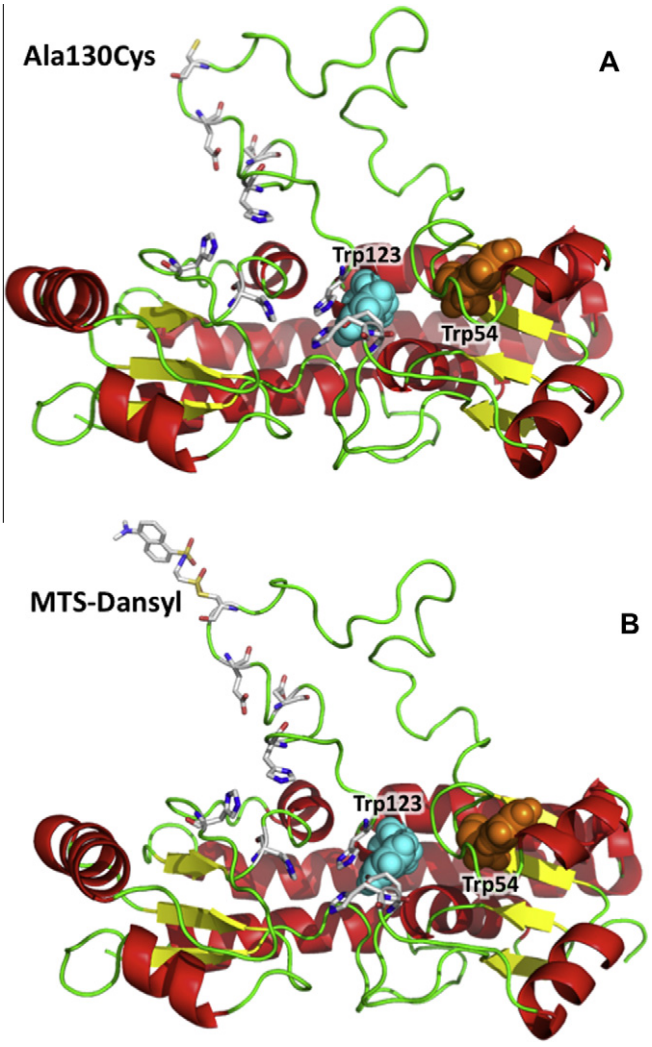

Fig. 1. (A) Cartoon diagram of the apo, Ala130Cys mutant, Se–ZnuA model. The α-helices are indicated by red spirals while the β-strands are represented by yellow arrows. Random coil and turns are shown as a green wire, the tryptophan residues are indicated by the spacefill models and the residues involved in the zinc coordination are shown by the stick representation. (B) Cartoon diagram of the apo, Se–ZnuA model with the MTS-Dansyl probe linked on Cys130. These pictures have been obtained using the PyMol program [18]. (For interpretation of the references to colour in this figure legend, the reader is referred to the web version of this article.)

plasmid [5] codifying for ZnuA protein under the control of an inducible promoter. The sequence of the mutated plasmid, named p18PznuA Ala130Cys, was confirmed by nucleic acid sequencing.

This mutant was specifically labeled with dansylamidoethyl methanethiosulfonate (StZnuA A 130C-DMTS) (Fig. 1B), that has been used as a probe in the fluorescence experiments.

E. coli DH5 cells were independently transformed with p18PznuA and p18PznuA Ala130Cys to respectively produce ZnuA wild-type and ZnuA Ala130Cys mutated proteins, as previously described [5]. Briefly, the transformed cells were grown overnight in LB medium at 37 °C and 120 RPM, in the presence of 1 mM IPTG. The cells were harvested by centrifugation for 15 min at 8000*g* and resuspended in 500 ml of isotonic solution. The periplasmic proteins were released by osmotic shock as already described [16]. After a 20 min centrifugation at 13,000 rpm, the periplasmic extract were applied to a Ni–nitrilotriacetic acid (Ni–NTA) column (Qiagen) pre-equilibrated with 50 mM sodium phosphate buffer, 250 mM NaCl, pH 7.8. The proteins were eluted with a discontinuous gradient of 0–250 mM imidazole. ZnuA eluted with 20–40 mM imidazole. The fractions containing ZnuA were pooled, dialyzed in 20 mM Tris–HCl, pH 7.0, and loaded on a HiLoad Q Sepharose fast-performance liquid chromatography (FPLC) column (Pharmacia Biotech) pre-equilibrated with 20 mM Tris–HCl, pH 7.0. Elution was performed using a 0–400 mM NaCl linear gradient. The peak fractions corresponding to ZnuA protein were further purified by a gel-filtration column (HiLoadTM 16/60 Superdex 75) equilibrated with 20 mM HEPES, 10 mM NaCl, pH 7.0. The protein concentration was determined by UV spectroscopy using a coefficient of ε_{280} - nm = 24410 M^{-1} cm^{-1} at 280 nm.

2.3. Labeling of Ala130Cys ZnuA with DMTS

The recombinant Ala130Cys ZnuA was incubated with 2 mM DTT and, after removal of the reductant by size-exclusion chromatography, labeled with excess of DMTS a probe that reacts selectively with the cysteine residues. The unreacted label was removed by gel-filtration on an FPLC apparatus with a Fast Desalting column HR 10/10 (Amersham-Pharmacia, Milan, Italy) eluted with 20 mM HEPES, 100 mM NaCl, pH 7.0.

Metal-free ZnuA proteins were produced by dialyzing the wild-type and the labeled mutant protein for 12 h against 50 mM sodium acetate buffer pH 5.5, in the presence of 1 mM EDTA followed by a further dialysis against 50 mM sodium acetate pH 5.5, 0.1 M NaCl to remove excess EDTA. The proteins were dialysed in 20 mM HEPES, 100 mM NaCl, pH 7.0 and stored at 4 °C until use. The labeled protein was analyzed for its protein content by absorbance at 280 nm, using an extinction coefficient of ε_{280} - nm = 24410 M^{-1} cm^{-1} at 280 nm, estimated from the protein sequence according to [17]. The contribution of DMTS to the absorption at 280 nm was estimated by the absorption value at 335 nm multiplied by 0.423 and subtracted from the total absorbance before calculation of protein concentration. The 0.423 correction factor was obtained from the ratio of absorbances at 280 and 335 nm of a 10 μM water solution of DMTS, after reaction with a 10-times molar excess of β-mercaptoethanol. From this same solution, we estimated an extinction coefficient of ε_{335} - nm = 3500 M^{-1} cm^{-1} for DMTS. According to these values, the average number of DMTS molecules per protein was between 0.7 and 0.9 for different protein preparations.

2.4. Fluorescence experiments

Fluorescence experiments were performed with a Fluoromax-4 (Horiba, Japan) photon counting fluorimeter, equipped with automatic Glan–Thompson polarizers. Temperature was controlled to 20 °C, within 0.1 °C, with a thermostated cuvette holder. Intrinsic fluorescence of the wild-type protein was measured with the following parameters: λ_{ex} at 295 nm (bandwidth of 5 nm), λ_{em} at 350 nm (bandwidth of 5 nm), and a 320 nm cutoff filter. DMTS fluorescence was measured with λ_{ex} at 330 nm (bandwidth of 7 nm), λ_{em} at 514 nm (bandwidth of 7 nm). Each anisotropy value is the result of 9 replicate measurements, with a 4 s averaging time for each polarizer orientation. A 3 μM protein solution was titrated with increasing amounts of Zn^{2+}.

3. Results

3.1. Fluorescence experiments

Fig. 2 shows the variation in emission intensity and anisotropy of the intrinsic fluorescence due to the presence of Trp54 and Trp123 at the base of the His-loop of wild-type ZnuA, as a function of Zn^{2+} concentration. For both parameters a linear variation is observed up to a Zn^{2+} concentration equimolar to that of the protein, with an increase in the intensity and a decrease in anisotropy indicative of a perturbation due to the binding of a zinc ion with very high affinity. No significant changes were observed at higher zinc concentrations.

Fig. 3 reports the variations in intensity and anisotropy of fluorescence for a DMTS fluorophore attached to a cysteine residue substituting Ala130. In this case a slight linear decrease is observed in both quantities up to an equimolar Zn^{2+} concentration, confirming the presence of one zinc binding site with high affinity. After this concentration, both the intensity and the anisotropy increase significantly, with a behavior corresponding to a second binding equilibrium with a dissociation constant of the order of 1 μM. In Fig. 3 the data has been reported at a single wavelength, but in the performed experiments the whole spectrum has been collected using a "magic angle" orientation of the polarizers to avoid polarization artifacts. A minimal spectral shift has been identified (from

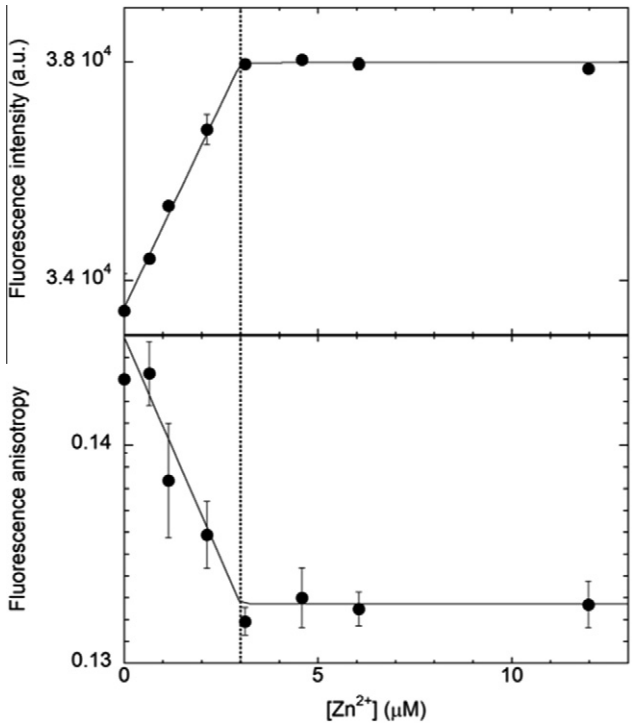

Fig. 2. Variation in the intrinsic fluorescence intensity (upper panel) and anisotropy (lower panel) of WT ZnuA as a function of added Zn^{2+} concentration. ZnuA concentration was 3 μM, and conditions of equimolarity are indicated by a vertical dotted line.

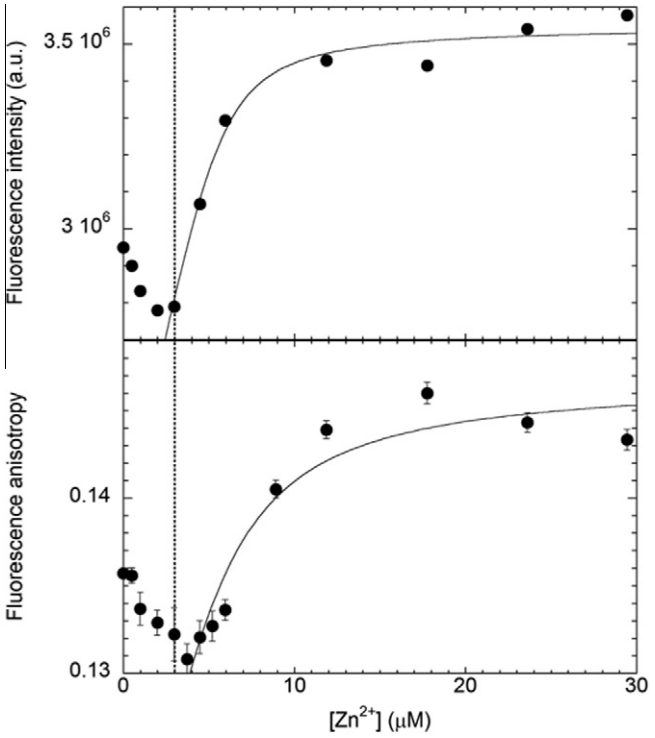

Fig. 3. Variation in the fluorescence intensity (upper panel) and anisotropy (lower panel) of DMTS attached to A 130C ZnuA, as a function of added Zn^{2+} concentration. ZnuA concentration was 3 μM, and conditions of equimolarity are indicated by a vertical dotted line.

about 517–512 nm) and the overall intensity increased similarly to the intensity measured at 514 nm (see Fig. 1S of Supplementary material).

The fluorescence data indicate that ZnuA has two Zn^{2+} binding sites. One of them has a very high affinity, so that, under the conditions used in the present experiments, all the added Zn^{2+} ions are stoichiometrically bound. Binding to this site significantly influences the emission intensity of ZnuA Trp residues (Fig. 4A), indicating that the ion binds in a cleft that modifies the environment surrounding these side chains. Binding of zinc also induces a reduction in the steady-state anisotropy, but this can be due either to a reduced fluorophore dynamics, or to an increase in the lifetime of the fluorophore's excited-state. Since Zn^{2+} binding causes also an increase in fluorescence intensity (which is probably associated to an increase in lifetime), the present data do not allow us to determine if the decrease in fluorescence anisotropy is due just to this effect, or also to a variation in the Trp dynamics.

Binding to the second site occurs with a dissociation constant of the order of 1 μM. This binding can not be monitored following the Trp fluorescence property but only by a fluorophore attached to residue 130 (Fig. 4B). In this case, a concomitant increase in both fluorescence anisotropy and intensity is observed, indicating a binding-induced reduction in the flexibility of the loop where the probe is attached, suggesting that the second Zn^{2+} ion binding site is located on the His-loop.

The affinities for the tight binding site is so high that, under the experimental conditions employed, all added Zn^{2+} will bind to that site until a 1:1 stoichiometry is reached. Therefore, there is essentially no ion free in solution that could stably interact with the weak binding site, until the tight binding site is saturated. The binding constant for the second site was thus determined by using only the data points with total ligand concentration higher than that of the protein.

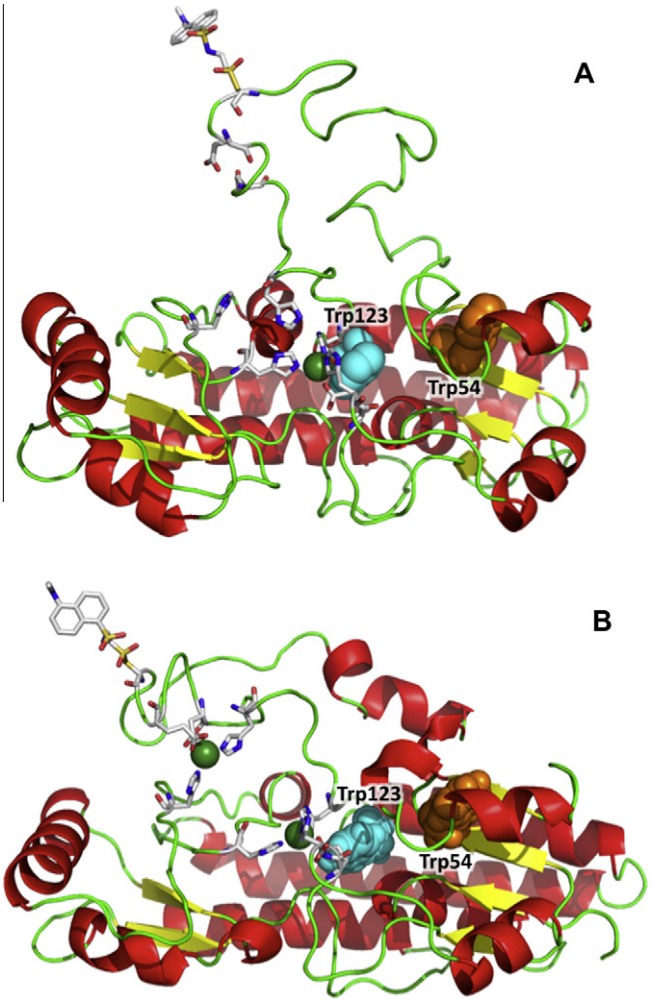

Fig. 4. (A) Cartoon diagram of the Se–ZnuA model with the MTS-Dansyl probe linked on Cys130 and the first, high affinity, site filled by a zinc ion. The structure is shown as described in the legend of Fig. 1 with the zinc metal represented by a green sphere. (B) Cartoon diagram of the Se–ZnuA model with the MTS-Dansyl probe linked on Cys130 and the two sites, the first with high affinity close to the tryptophan residues and the second with low affinity on the His-loop, filled by zinc ions. These pictures have been obtained using the PyMol program [18].

3.2. Structural considerations

The *S. enterica* homology models, hypothesized in a previous paper by Falconi and coworkers [14], fit very well with these spectroscopic findings. The two models named DZn1 and DZn2, each containing two zinc ions, show an identical primary zinc site composed by one Glu and three His residues (Glu59, His60, His147 and His211), located at the base of the His-loop and in proximity of the Trp residues, as observed in the *E. coli* ZnuA template [10], while the second zinc ion was bound to residues Glu132, Asp136, His141 and His228 in the DZn1 model and to residues Glu124, Glu133, His139 and His228 in the DZn2 model [14]. The two modeled secondary sites share a common ligand, His228 that does not belong to the His-loop but is suggested as a ligand also in the X-ray diffraction study of *E. coli* protein [10]. In the 3D ZnuA structure from *S. enterica* [11] the primary zinc binding site is located in proximity of the Trp residues with a coordinating residue coming from His-loop (His140 in the place of His60, used as a ligand in the models [14]), that is very improbable as a stable ligand of the primary zinc site, since binding of the first zinc doesn't induce a reduction of the mobility of the fluorophore located in the His-

loop. It is then likely that the structure detected by the X-ray diffraction represents an intermediate state, possibly favored by the low metallation of the protein sample used in crystallographic experiments [11], in the process of transferring the Zn^{2+} ion from the secondary to the primary zinc site.

In the previous modeling study the ZnuA models containing one and two zinc ions have been also sampled by molecular dynamics simulation [14]. Calculation of Ala130 average fluctuations, i.e. of the residue experimentally mutated in cysteine and then linked to the fluorophore, indicates a moderate fluctuation when the primary site is loaded with a single zinc ion (average RMSF about 0.5), that are strongly reduced when the secondary zinc site is filled (average RMSF about 0.2). As indicated by the results of the intrinsic fluorescence (Fig. 2), our model confirms the presence of the first, high affinity, zinc binding site located in the proximity of the two Trp residues (Trp54 and Trp123) and the involvement of the His-loop in the DMTS fluorescence analysis (Fig. 3) indicates the presence of a stable second binding site provided with lower zinc affinity. The length, together with the extreme flexibility of the His-loop, make it unlikely that the presence of the extrinsic fluorescent probe may alter the intrinsic binding affinity of the ZnuA protein.

4. Discussion

The intrinsic fluorescence data suggest that StZnuA interacts with a first zinc ion with a very high association constant ($K_d \ll 0.1$ μM) (Fig. 2) and subsequently with one or more metal ions with a lower affinity ($K_d \sim 1.0$ μM) (Fig. 3). The two association processes are responsible for different structural effects because only the first influences the fluorescence of the protein Trp residues (Fig. 2), while the emission of DMTS is mostly affected by the second (Fig. 3). The different structural effects due to the two association events are confirmed by steady-state fluorescence anisotropy, which determines the rotational dynamics of the fluorescent probe during its excited state lifetime. Fig. 3 shows a decrease in anisotropy as a result of the stoichiometric interaction of the first ion and no significant change for the next process. Although in this case the anisotropy decrease could be due just to a variation in the excited-state lifetime of the Trp residues (indicated by their fluorescence intensity increase) it is possible to exclude this possibility for DMTS fluorescence data. In fact, in this case the second binding process causes increase in both fluorescence anisotropy and intensity (Fig. 3), so that the anisotropy variation is necessarily associated to a reduction in DMTS mobility.

Overall these effects can be explained with two conformational changes, due to the binding of the Zn^{2+} ions. In particular the first interaction is felt mostly by tryptophans, while the second one acts substantially on DMTS. These binding events are responsible of changes in the polarity of the environment surrounding the probes and they affect their mobility.

On the basis of the data obtained and the protein models proposed we hypothesize a mechanism in which the His-loop can be permanently loaded with zinc only when the primary site is filled. The bound zinc ion may actually lend structure to the His-loop, allowing the interaction of ZnuA with ZnuB, the membrane transporter of the ABC system. The mechanism that we propose gives an explanation for the data obtained through the fluorescence experiments and opens the way for further experiments performed to abolish the ZnuA–ZnuB interaction and to determine the identity of the ligands that shape the second ZnuA zinc binding site.

Acknowledgments

This work was supported by a Grant from the Fondazione Roma.

Appendix A. Supplementary data

Supplementary data associated with this article can be found, in the online version, at http://dx.doi.org/10.1016/j.bbrc.2012.11.073.

References

[1] C. Andreini, L. Banci, I. Bertini, A. Rosato, Counting the zinc-proteins encoded in the human genome, J. Proteome Res. 5 (2006) 196–201.
[2] C. Andreini, I. Bertini, G. Cavallaro, G.L. Holliday, J.M. Thornton, Metal ions in biological catalysis: from enzyme databases to general principles, J. Biol. Inorg. Chem. 13 (2008) 1205–1218.
[3] K. Hantke, Bacterial zinc uptake and regulators, Curr. Opin. Microbiol. 8 (2005) 196–202.
[4] S. Patzer, K. Hantke, The ZnuABC high-affinity zinc-uptake system and its regulator Zur in Escherichia coli, Mol. Microbiol. 28 (1998) 1199–1210.
[5] P. Petrarca, S. Ammendola, P. Pasquali, A. Battistoni, The Zur-regulated ZinT protein is an auxiliary component of the high affinity ZnuABC zinc transporter that maximize metal recruitment during severe zinc shortage, J. Bacteriol. (2010) 1553–1564.
[6] S. Ammendola, P. Pasquali, C. Pistoia, P. Petrucci, P. Petrarca, G. Rotilio, A. Battistoni, The high affinity Zn^{2+} uptake system ZnuABC is required for bacterial zinc homeostasis in intracellular environments and contributes to virulence of *Salmonella enterica*, Infect. Immun. 75 (2007) 5867–5876.
[7] J.Z. Liu, S. Jellbauer, A. Poe, V. Ton, M. Pesciaroli, T. Kehl-Fie, N.A. Restrepo, M. Hosking, R.A. Edwards, A. Battistoni, P. Pasquali, T.E. Lane, W.J. Chazin, T. Vogl, J. Roth, E.P. Skaar, M. Raffatellu, Zinc sequestration by the neutrophil protein calprotectin enhances *Salmonella* growth in the inflamed gut, Cell Host Microbe 11 (2012) 227–239.
[8] J.P. Claverys, A new family of high-affinity ABC manganese and zinc permeases, Res. Microbiol. 152 (2001) 231–243.
[9] S. Banerjee, B. Wei, M. Bhattacharyya-Pakrasi, H.B. Pakrasi, T.J. Smith, Structural determinants of metal specificity in the zinc transport protein ZnuA from synechocystis 6803, J. Mol. Biol. 333 (2003) 1061–1069.
[10] L.A. Yatsunyk, J.A. Easton, L.R. Kim, S.A. Sugarbaker, B. Bennett, R.M. Breece, Vorontsov II, D.L. Tierney, M.W. Crowder, A.C. Rosenzweig, Structure metal binding properties of ZnuA, a periplasmic zinc transporter from *Escherichia coli*, J. Biol. Inorg. Chem. 13 (2008) 271–288.
[11] A. Ilari, F. Alaleona, P. Petrarca, A. Battistoni, E. Chiancone, The X-ray structure of the zinc transporter ZnuA from *Salmonella enterica* discloses a unique triad of zinc-coordinating histidines, J. Mol. Biol. 409 (2011) 630–641.
[12] B. Wei, A.M. Randich, M. Bhattacharyya-Pakrasi, H.B. Pakrasi, T.J. Smith, Possible regulatory role for the histidine-rich loop in the zinc transport protein ZnuA, Biochemistry 46 (2007) 8734–8743.
[13] D.C. Desrosiers, Y.C. Sun, A.A. Zaidi, C.H. Eggers, D.L. Cox, J.D. Radolf, The general transition metal (Tro) and Zn^{2+} (Znu) transporters in Treponema pallidum: analysis of metal specificities and expression profiles, Mol. Microbiol. 65 (2007) 137–152.
[14] M. Falconi, F. Oteri, F. Di Palma, S. Pandey, A. Battistoni, A. Desideri, Structural-dynamical investigation of the ZnuA histidine-rich loop: involvement in zinc management and transport, J. Comput. Aided Mol. Des. 25 (2011) 181–194.
[15] G. Berducci, A.P. Mazzetti, G. Rotilio, A. Battistoni, Periplasmic competition for zinc uptake between the metallochaperone ZnuA and Cu, Zn superoxide dismutase, FEBS Lett. 569 (2004) 289–292.
[16] S. Ammendola, P. Pasquali, F. Pacello, G. Rotilio, M. Castor, S.J. Libby, N. Figueroa-Bossi, L. Bossi, F.C. Fang, A. Battistoni, Regulatory and structural differences in the Cu, Zn-superoxide dismutases of *Salmonella enterica* and their significance for virulence, J. Biol. Chem. 283 (2008) 13688–13699.
[17] C.N. Pace, F. Vajdos, L. Fee, G. Grimsley, T. Gray, How to measure and predict the molar absorption coefficient of a protein, Protein Sci. 4 (1995) 2411–2423.
[18] W.L. DeLano, The PyMOL Molecular Graphics System, DeLano Scientific, San Carlos, CA, USA, 2002 (http://wwwpymolorg).